ISSN 2638-1451

Clinics of Surgery

Research Article

Hybrid Strategy of Cervical Artificial Disc and Intervertebral Cage – Biomechanical Effects on the Adjacent Tissues and Implants

Chung TT[1,2,4], Hueng DY[2], Hsu CP[3], Chen CM[3] and Lin SC[3*]

[1]Department of Surgery, Graduate Institute of Applied Science and Technology, National Taiwan University of Science and Technology, Taipei, Taiwan

[2]Department of Neurological Surgery, Tri-Service General Hospital, National Defense Medical Center, Taipei, Taiwan

[3]Department of Surgery, Graduate Institute of Biomedical Engineering, National Taiwan University of Science and Technology, Taipei, Taiwan

[4]Department of Surgery, Cheng Hsin General Hospital, Taipei, Taiwan

Volume 3 Issue 3- 2020

Received Date: 13 Aug 2020

Accepted Date: 14 Sep 2020

Published Date: 21 Sep 2020

2. Key words

Cervical degeneration; Finite element; Hybrid surgery, ASD, ACDF, C-ADR

1. Abstract

1.1. Background: Hybrid surgery with Cervical Artificial Disc Replacement (C-ADR) and Anterior Cervical Discectomy and Fusion (ACDF) are an alternative treatment to reduce the level of increased rigidity, but biomechanical differences between strategies using one C-ADR and two ACDFs have not been thoroughly investigated.

1.2. Methods: A nonlinear finite element model from the C2 to the T1 vertebrae was developed. Ligament interconnection, follower loads, and weight compression were used to simulate cervical flexion. Within the C4-C7 segments, two placements of one C-ADR and two ACDFs were arranged: PAP (peek cage, artificial disc, and peek cage) and APP.

1.3. Results: Both PAP and APP consistently induced kinematic and mechanical redistribution to adjacent segments. The C-ADR served as a buffer of the compensated motion and stress from the ACDF segments. The motion and stress of the cranial C2-C3 and C3-C4 segments were greater for the PAP than the APP constructs. However, the caudal C7-T1 segment of the APP construct was more flexed and stressed. Serially stacked cages of the APP placement increased bone-cage stresses, potentially inducing subsidence and loosening. The sandwiched C-ADR of the PAP construct accommodated the compensated motion and stress from the adjacent ACDFs more than the APP construct.

1.4. Conclusions: The PAP and APP placements cause more severe ASD progression at the cranial and caudal segments, respectively. The PAP placement is preferred for concerns regarding ACDF and postoperative degeneration of caudal segments. The APP placement is recommended when C-ADR failure and ASD progression are considered.

3. Abbreviations

C-ADR: Cervical Artificial Disc Replacement; ACDF: Anterior Cervical Discectomy and Fusion; ASD: Adjacent Segment Degeneration; P: Peek Cage; A: Artificial Disc; CT: Computed Tomography; ROM: Range-Of-Motion; HS: Hybrid Surgery

4. Introduction

Hybrid surgery using C-ADR and ACDF has been extensively applied in the multilevel treatment of cervical instability and degeneration [1-4]. However, cervical motion is influenced adversely as more levels are incorporated into the instrumentation. The design rationale for artificial disc (i.e. dynamization) and intervertebral cage (i.e. fusion) are quite different when treating cervical instability. Therefore, for different placements of artificial discs and intervertebral cages, levels adjacent to instrumentation may experience different degeneration. For C4-C7 instrumentation, two strategies for placing one artificial disc (A) and two peek cages (P), as APP and PAP, are described in the literature [5-7]. In the APP construct, the C4-C5 segment is instrumented by C-ADR, followed by two ACDFs at the C5-C6 and C6-C7 segments. In the PAP construct, the C-ADR is instrumented at the C5-C6 segment and the ACDF are used in two adjacent C4-C5 and C6-C7 segments.

***Corresponding Author (s):** Shang-Chih Lin, Department of Surgery, Graduate Institute of Biomedical Engineering, National Taiwan University of Science and Technology, No.43, Section 4, Keelung Road, Taipei, 10607, Taiwan Tel: +886-2-8792-7177, Fax:+886-2-8792-7178, E-mail: ztc1979@yahoo.com.tw*

Citation: Lin SC, Hybrid Strategy of Cervical Artificial Disc and Intervertebral Cage – Biomechanical Effects on the Adjacent Tissues and Implants.Clinics of Surgery. 2020; 3(3): 1-7.

There are two hypotheses proposed in this study: a boundary effect and a trade-off concept. For the APP construct, the C-ADR is placed between two cranially intact and two caudally fused segments. However, for the PAP construct, the C-ADR is sandwiched by two fused segments. This study hypothesized that different boundaries theoretically affect the articulation of the artificial disc to induce dissimilar responses to adjacent tissue degeneration and vertebral-implant outcomes. This implies that the strategies of placing one rotatory C-ADR and two rigid ACDF potentially alter the biomechanical properties of the hybrid construct [8, 9].

Problems induced by two implants in multilevel instrumentation are reported: Adjacent Segment Degeneration (ASD) [2, 4, 10, 11] and mechanical failure of the bone-implant construct [12-14]. The distinguishable characteristics of rotary C-ADR and fusion ACDF may show different responses to multilevel instrumentation [11, 13, 14]. Consequently, the trade-off concept hypothesizes that the rationale of optimal instrumentation should be a compromise between the ASD problem and implant failure [15]. To the current authors' knowledge, no study has yet clarified how implant-induced problems between the PAP and APP strategies are different.

This study aimed to investigate the biomechanical differences between the APP and PAP placement for C4-C7 instrumentation. A cervicothoracic model with physiological loads and degenerative segments was developed and validated to evaluate the effects of the two hybrid strategies on tissue responses and implant outcomes. The surgical criteria for the PAP and APP placements are discussed in terms of the ASD progression and implant failure. The findings of the current study may provide an insight into three-level instrumentation using C-ADR and ACDF as treatment for cervical degeneration.

5. Materials and Methods

5.1. Development of a Nonlinearly Cervicothoracic Column

This study used the published finite-element model by the current authors [16]. It was established an osseo-ligamentous cervicothoracic model from C2 to T1 segments using Computed Tomography (CT) of a 55-year-old male volunteer without any cervical disease. The CT images of his cervicothoracic column with 1-mm transverse slice separation were reconstructed in three dimensions with triangular surface meshes using PhysiGuide software, version 2.3.1 (Pou Yuen Technol8ogy Co., Changhua, Taiwan). The surface meshes were further transformed into a solid model with smooth and seamless surfaces by using Solid Works software, version 2018 (Solid Works Corporation, Concord, MA, USA).

The cervicothoracic model consisted of vertebral bodies, posterior bony elements, endplates, intervertebral discs, and surrounding ligaments (Figure 1). Vertebral body were composed of a cortical shell and a cancellous core. The articulating surfaces of the paired facet joints were cautiously prepared to ensure interfacial contact during excessive motion. The curved gaps of the healthy facet joint were consistently 0.5 mm in an unloaded neutral position [17]. The endplate was modeled as a 1-mm plate, sandwiched between the vertebral body and intervertebral disc. An intervertebral disc consisted of an annular fibrosus and a nucleus pulpous. The annulus fibrosus was modeled as a hyper elastic composite [18], while the nucleus pulpous was simulated as a cavity filled with non compressive fluids.

The ligaments included the anterior longitudinal ligament, posterior longitudinal ligament, supraspinous ligament, interspinous ligament, inter transverse ligament, ligamentum flavum, and facet capsular ligament. The ligaments were modeled as the tension-only springs to join their attachment points on adjacent vertebrae (Table 1). The insertions and origins of the ligaments on the right and left sides were assumed symmetrical with respect to the sagittal plane. Except for the cancellous core, the constitutive laws of all bony tissues were assumed to be linearly elastic and isotropic. The material properties of bones, endplates, discs, and ligaments were obtained from the literature (Table 1) [17-19].

The C4-C7 segments were simulated as moderate degeneration with the height reduced by 33%, the annulus area expanded by 40%, the nucleus modulus increased by 66%, and the facet gap decreased by 0.3 mm because of dehydration (Figure 2A) [20]. For the PAP construct, the artificial disc was instrumented into the C5-C6 segment and the peek cages were inserted to the C4-C5 and C6-C7 segments. For the APP construct, the C4-C5 segment was instrumented with an artificial disc and two peek cages were removed to the C5-C7 segments (Figure 2C).

The artificial disc and intervertebral cage used in this study were the Prestige LP Cervical Disc System (Medtronic Sofamor Danek, Memphis, TN, USA) and Cervios system (Synthes, Paoli, PA, USA). The spikes of the cages were neglected for computational efficiency (Figure 1B). Placement of the artificial disc and peek cages were monitored by an orthopedic surgeon. This study used the terms "cranial" and "caudal" to denote the different cages and adjacent (C3-C4 and C7-T1) segments, respectively (Figures. 2B and 2C).

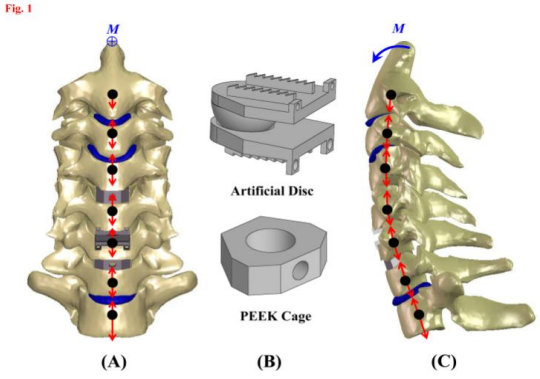

Figure 1: A nonlinear cervicothoracic model with three-dimensional networks of ligament interconnection, follower loads, and weight compression. (A) Front view. (B) Cervical implants. (C) Lateral view.

Table 1: Material and geometric properties of spine tissues and implants

Material	Elastic Modulus (MPa)		Poisson's Ratio (dimensionless)	Cross-sectional Area (mm2)	References
Bones					[16-18]
Cortical Shell	10,000		0.3	–	
Cancellous Core	450		0.25	–	
Posterior Element	3,500		0.25	–	
Endplate	500		0.4	–	
Disc					[16,17,19]
Annulus Fibrosus	c_1	c_2		Depends on Levels and Degeneratio	
	0.2 (Healthy)	0.05 (Healthy)	–		
	0.9 (Grade II)	0.23 (Grade II)	–		
Nucleus Pulposus	1.00 (Healthy)		0.499 (Healthy)	Depends on Levels and Degeneratio	
	1.66 (Moderate Grade)		0.4 (Moderate Grade)		
Ligaments					[16]
Anterior Longitudinal	15 (<12%) 30 (>12%)		–	33	
Posterior Longitudinal	10 (<11%) 20 (>12%)		–	33	
Inter-spinous	5 (<25%) 10 (>25%)		–	13.1	
Ligamentum Flavum	7 (<12%) 30 (>12%)		–	50.1	
Facet Capsular	15 (<40%) 30 (>40%)		–	46.6	
Implants					[18,22]
PEEK	3,600		0.3	–	
CoCrMo Alloy	210,000		0.3	–	

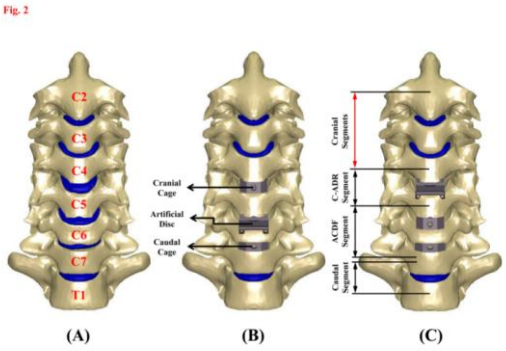

Figure 2: Three finite-element constructs investigated in this study. (A) Intact construct. (B) PAP construct. (C) APP construct.

5.2. Finite-element Analyses

The bottom surface of the T1 vertebral body was fully constrained and the cervicothoracic column was flexed by the follower and concentrated loads (Figure 1). The follower loads (73.6 N) were used to stabilize the cervicothoracic column and simulated by the tube–slider–cable mechanism in which the slider could slide along the tube hole and the springs were connected piece-by-piece by the sliders [19]. The tubes were placed at optimal sites posterior to the center of each vertebral body [21]. The pulling load was exerted at the cable end in the tangential direction of the cable curve. The concentrated loads (1.0-Nm moment) were driven from the head weight and muscular contractions, and applied at the cervicothoracic end [19]. Using the displacement-controlled method [22], the criterion for controlling the same motion was adopted as a reasonable approach for evaluating the implant-induced effects on the adjacent segments and implants.

The interfaces of facet joints and artificial disc were modeled as the surface-to-surface contact elements, which allow separation and slippage thereby reducing friction [16, 17]. The other interfaces between implants and tissues were assumed to be bonded. All implant materials were assumed to have linearly elastic, homogeneous, and isotropic material properties throughout (Table 1). The calculated von Mises stresses of all implants were compared with the yielding strength of the corresponding material to validate the assumption of linear elasticity.

An automatic algorithm was used to generate the ten-node tetrahedral solid elements to mesh the cervicothoracic constructs. The mesh refinement was locally controlled at the high stress-concentrated sites and articulating surfaces. Using an aspect ratio and a Jacobian check, the quality of all elements was monitored to avoid sharp discontinuities and unrealistically high stress concentrations. Mesh refinement was conducted for modeling accuracy until excellent monotonic convergence behavior with <5% difference in the total strain energy was achieved. A nonlinear algorithm with a large-deformation formula and direct-sparse solver was used via Solid Works simulation software.

5.3. Validation of the Finite-element Model

Experimental and numerical comparisons were used to validate the simplifications and assumptions of the current model. Using the experimental and numerical data of Kallemeyn et al. [18], the assumed loads (1.0 Nm) were exerted onto the cervicothoracic top of the C2-C7 model to calculate the cervical range-of-motion (i.e. disc angle) of the current model. The calculated results were validated by the total disc angles for flexion, extension, bending, and rotation. For the facet forces, the current C3-C6 model was validated by the extension data of Jung et al. [19] During the validation, the initially chosen elastic module of the disc and some ligaments were slightly modified within the physiological range to improve the consistency with the cadaveric results.

Five indices were chosen to evaluate the effects of the hybrid strategy on the adjacent tissues and implants, including disc angles, disc stresses, facet forces, cage stresses, and stress and articulation of artificial disc. The von Mises stress was used as the index of the equivalent stress in this study. The disc and cage stresses were defined as the average value of the stresses within the overall disc and cage, respectively. The facet force was the sum of normal contact at the right and left facet joints. After flexion, the articulation of the artificial disc was defined as the relative slippage of the articulating surfaces.

6. Results

6.1. Validation of the Finite-element Model

After slightly modifying the elastic moduli of the disc and ligaments, this study had been validated and published to achieve a good agreement (Figure 3) [16]. For the intact model, the ROM error of the current and cadaveric results was 6.3% for flexion, 7.5% for extension, 7.2% for bending, and 3.9% for rotation (Figure 3A). The predicted cervical ROMs for all levels were within one standard deviation of the Kallemeyn data [17]. For the numerical validation [17], the cervical ROM error was 8.4% for flexion, 5.2% for extension, 9.6% for bending, and 7.2% for rotation (Figure 3B). The average error of the cervicothoracic motions was 4.7% for the experimental and 7.6% for numerical validation. The current model was validated for further analyses.

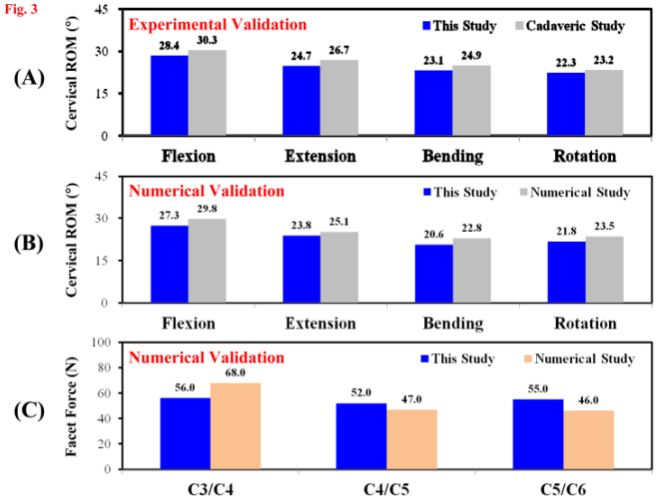

Figure 3: The predicted results of the current study are validated in terms of segmental ROM and fact force. (A) Comparison with the cadaveric results[16]. (B) and (C) Comparison with the numerical results[16,17]

6.2. Tissue Responses

For the intact and instrumented constructs, the kinematic and mechanical data of the adjacent segments were shown in the picture (Figure 4). Both strategies consistently increased the motion and load demands of the adjacent discs and facet joints. On average, the cranial disc angles were 27.6%, stresses were 27.5%, and facet forces were 23.9% for the PAP construct; and were 13.5%, 13.4%, and 10.6%, respectively, for the APP construct, being greater than those of the intact construct. At the caudal segments, the PAP and APP constructs increased by 24.4% and 51.2%, respectively, for disc angle, 5.9% and 17.6%, respectively, for disc stress, and 15.3% and 34.0%, respectively, for facet force compared to the intact construct.

Between hybrid strategies, the cranial segments of the PAP construct were more flexed and loaded than the APP construct. For the PAP construct, the disc angles of the C2-C3 and C3-C4 segments were 4.1% and 21.3%, respectively, and greater than those of the APP construct (Figure 4A). Similarly, the increases in the cranial segments were 18.2% and 7.1%, respectively, for disc stress and 10.1% and 5.5%, respectively, for facet force (Figures. 4A and 4C). The motion and load of the caudal segment (C7-T1) were more compensated for the APP than the PAP constructs. The disc angle, disc stress, and facet force of the APP construct were 21.6%, 11.1%, and 16.2%, respectively, greater than those of the PAP construct.

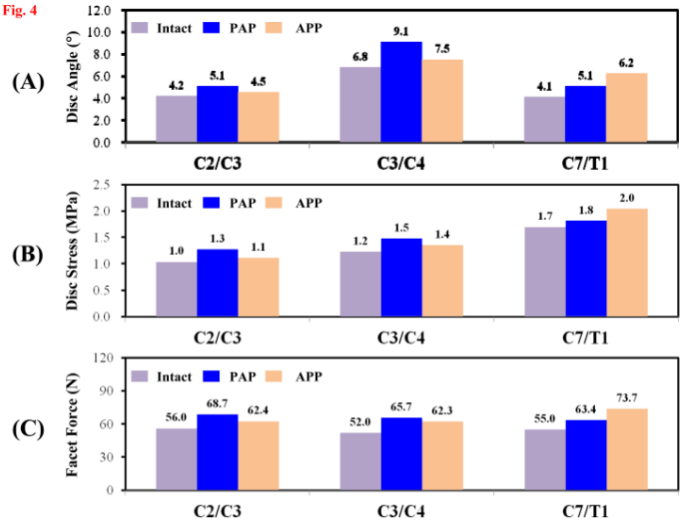

Figure 4: The kinematic and mechanical compensation from the instrumented to adjacent segments. (A) Disc ROM. (B) Disc stress

6.3. Implant Behaviors

The kinematic and mechanical data of the ACDR and C-ADR are shown in the picture (Figure 5). The cage stresses of the APP construct were consistently greater than those of the PAP construct. The cranial and caudal cages of the APP construct had more stress than the corresponding values of the PAP construct by 28.6% and 16.7%, respectively (Figure 5A). However, the C-ADR stress of the PAP construct was 23.5% greater than that of the APP construct (Figure 5B). The artificial discs of the two strategies showed the concentrated articulation at the C-ADR interfaces than the intact disc (Figure 5C). At the C5-C6 segment, the C-ADR angle of the PAP construct was increased by 76.0%, while that of the APP construct was 16.7%, which was greater than that of the intact C4-C5 segment. Between the two strategies, the artificial disc of the PAP construct was more flexed, about 11.0% greater than that of the APP construct.

7. Discussion

7.1. Biomechanical Effects of the APP and PAP Placements

After hybrid surgery with ACDF and C-ADR, the peek cage fuses the inter segmental disc, while the artificial disc allows for intervertebral motion (Figure 5C). If the same range of cervical motion is desired, the constrained mobility of the fused segments will be transferred to the adjacent segments and flexible implants. From a biomechanical viewpoint, this indicates where the C-ADR around the ACDF segment will have a significant effect on tissue responses

and implant behavior (Figures 4 and 5). The motion-buffering concept is used to schematically illustrate the biomechanical differences between the PAP and APP placements (Figure. 6).

Fig. 5

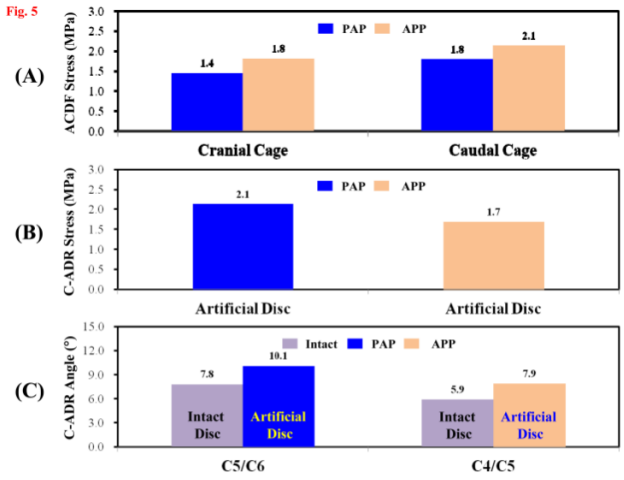

Figure 5: The stress values of the peek cages and artificial disc. (A) Cage stress. (B) Artificial disc stress.

For the PAP construct (Figure 6A), the constrained C4-C5 mobility imposed by the cranial cage is translated to both the cranial C3-C4 segment (i.e. APAP) and caudal C-ADR (i.e. BPAP). The articulation of the C-ADR components is freer than the deformation of the osseo-ligamentous C3-C4 segment (Figure 5C) [19]. The constrained ACDF mobility is more compensated to the C-ADR than the contiguous segment (i.e. BPAP > APAP). For the APP construct (Figure 6B), the C-ADR is directly superimposed over the cranial cage to potentially share more of the constrained ACDF mobility than the C3-C4 segment. The mobility-buffering effect of the C-ADR indicates BAPP > AAPP.

Fig. 6

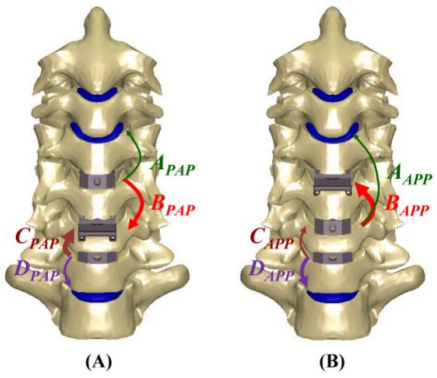

Figure 6: The mobility-buffering mechanisms to illustrate the biomechanical differenes between the two placements. (A) PAP construct. (B) APP construct.

Similarly, the caudal cage of the PAP construct transfers more mobility to the C-ADR than to the C7-T1 segment (i.e. CPAP > DPAP). However, the two stacked cages make the constrained mobility of the caudal cage more compensated to the C7-T1 segment than to the superimposed ACDF and C-ADR (DAPP > CAPP). These are used to discuss the biomechanical effects of the C-ADR and ACDF placements on tissue responses and implant behavior.

Tissue Responses

In general, the two placements consistently induce the kinematic and mechanical compensation of the contiguous C3-C4 and C7-T1 segments (Figure 4). The PAP placement shows greater increases in motion and stress of the cranial C2-C3 and C3-C4 segments than the APP placement. However, the two continuous cages of the APP construct inevitably concentrate the compensated motion and stress to the caudal C7-T1 segment. Consequently, the APP placement can be used in situations where there is a degenerative C3-C4, but healthy C7-T1 segment. The C-ADR at the C4-C5 segment buffers the ASD at the C3-C4 segment and the healthy C7-T1 segment tolerates the compensated motion and stress from two ACDF cages. If the cranial segments are healthy and the caudal segments are degenerative, the PAP placement is recommended because the flexible C-ADR buffers the compensated mobility from the cages on either side. However, the cranial cage still worsens the ASD problem of the cranial segments.

Implant Behaviors

The C-ADR and ACDF placements also have an important effect on the stress and motion of the adjacent implants (Figure 5). The two-level fusion of the APP placement consistently made the cages more highly stressed. For the PAP placement, the sandwiched C-ADR can serve as a mobility buffer (greater BPAP and CPAP) of the two fused segments, thereby effectively decreasing the cage stresses (Figure 5C). However, the greater amount (BPAP + CPAP) of the compensated mobility inevitably makes the C-ADR of the PAP construct more stressed than its counterpart (CAPP).

Between the two placements, differences in implant outcomes provide valuable information for the surgical planning of multilevel instrumentation. The APP placement is not recommended where there is poor bone quality that may result in ACDF loosening or subsidence. In comparison, the PAP placement should be cautiously evaluated if the postoperative complications of C-ADR wear and osteolysis are major concerns. The buffering ability of an artificial disc can make the APP more suitable for the initially obvious degeneration at cranial segments. PAP placement can be used when there are potential risks of progressive degradation of caudal segments.

Limitations of the Current Study

As with any finite-element model that attempts to simulate the cervicothoracic complexity, there are some limitations and underlying assumptions inherent in this study. Limited by data sources, the degenerative changes because of vertebral osteoporosis, facet osteoarthritis, endplate sclerosis, and annular tears are not included in this study. Their effects on the reported results were not independently and systematically investigated. Some studies found that the HS of C-ADR and ACDF is superior to ACDF only in terms of

better neck disability recovery, less postoperative neck pain, faster ROM recovery, and less adjacent ROM increase [1-3, 5, 7]. However, an exhaustive comparison between literature and the current study was not conducted because, to our knowledge, there is no previous report devoted to the biomechanical differences between the three-level PAP and APP placements. Experimental tests or long-term clinical evaluation should be conducted to validate the results of this numerical study.

In conclusion, there are two findings inherent in this biomechanical study of the PAP and APP placements (Figure 7). For the ASD problem, the PAP and APP placements definitely worsen the cranial and caudal segments, respectively. This provides surgical information that correlates the initial condition of the adjacent segments with the hybrid strategies. For the implant problem, the C-ADR mobility reduces the cage stresses of the PAP construct but accelerates C-ADR failure. Consequently, PAP placement should be considered when there is apprehension about ACDF subsidence and loosening. In turn, the APP placement is recommended in situations when C-ADR failure is considered.

Fig. 7

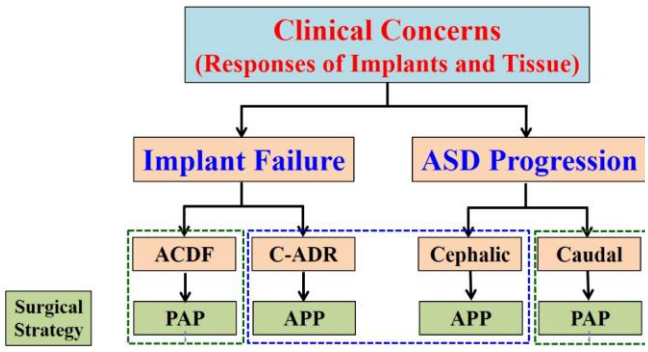

Figure 7: The recommended strategy of the PAP and APP surgeries.

8. Conclusions

C-ADR serves as a buffer for the compromised motion and stress from the ACDF. Therefore, the PAP and APP placements consistently worsen the ASD problem at the cranial and caudal segments, respectively. This study recommends the PAP placement is considered for apprehensions regarding ACDF problems and the degeneration of caudal segments. APP placement is recommended when C-ADR failure and ASD progression of cranial segments are considered.

9. Acknowledgements

The authors would like to thank the individuals, who participated in this simulative study.

References

1. Shin DA, Yi S, Yoon DH, Kim KN, Shin HC. Artificial disc replacement combined with fusion versus two-level fusion in cervical two-level disc disease. Spine 2009; 34: 1153-9.
2. Kelper CK, Brodt ED, Dettori JR, Albert TJ. Cervical artificial disc replacement versus fusion in the cervical spine: a systematic review comparing multi-level versus single-level surgery. Evid Based Spine Care J. 2012; 3:19-30.
3. Lee SB, Cho KS, Kim JY, Yoo DS, Lee TG, Huh PW. Hybrid surgery of multi-level cervical degenerative disc disease: review of literature and clinical results. J Korean Neurosurg Soc. 2012; 52: 452-8.
4. Jin YJ, Park SB, Kim MJ, Kim KJ, Kim HJ. An analysis of heterotrophic ossification in cervical disc arthroplasty: a novel morphologic classification of an ossified mass. The Spine J. 2013; 13: 408-20.
5. Ren X, Chu T, Jiang T, Wang W, Wang J, Li C, et al. Cervical disc replacement combined with cage fusion for the treatment of multi-level cervical disc herniation. Clin Spine Surg. 2016; 29: 218-25.
6. Hey HWD, Hong CC, Long AS, He HT. Is hybrid surgery of the cervical spine a good balance between fusion and arthroplasty? Pilot results from a single surgeon series. Eur Spine J. 2013; 22: 116-22.
7. Kang L, Lin D, Ding Z, Liang B, Lian K. Artificial disk replacement combined with mid-level ACDF versus multilevel fusion for cervical disk disease involving 3 levels. Orthopedics. 2013; 36: e88-94.
8. Daniels AH, Paller DJ, Feller RJ, Thakur NA, Biercevicz AM, Palumbo MA, et al. Examination of cervical spine kinematics in complex, multi-planar motions after anterior cervical discectomy and fusion and total disc replacement. Int J Spine Surg. 2012; 6: 190-4.
9. Wu XD, Wang XW, Yuan W, Liu Y, Tsai N, Peng YC, et al. The effect of multi-level anterior cervical fusion on neck motion. Eur Spine J. 2012; 21: 1368-73.
10. Nesterenko SO, Riley LH III, Skolasky RL. Anterior cervical discectomy and fusion versus cervical disc arthroplasty: current state and trends in treatment for cervical disc pathology. Spine 2012; 37: 1470-4.
11. Xia P, Chen HL, Cheng HB. Prevalence of adjacent segment degeneration after spine surgery: a systematic review and meta-analysis. Spine. 2013; 38: 597-608.
12. Gornet MF, Schranck FW, Taylor BA. Late subsidence after cervical disc arthroplasty. The Spine J 2012; 12: S83-4.
13. Gao Y, Liu M, Li T, Huang F, Tang T, Xiang Z. A meta-analysis comparing the results of cervical disc arthroplasty with anterior cervical discectomy and fusion (ACDF) for the treatment of symptomatic cervical disc disease. J Bone Joint Surg Am. 2013; 95: 555-61.
14. Nunley PD, Jawahar A, Kerr EJ, Gordon CJ, Cavanaugh DA, Birdsong EM, et al. Factors affecting the incidence of symptomatic adjacent-level disease in cervical spine after total disc arthroplasty: 2- to 4-year follow-up of 3 prospective randomized trials. Spine. 2012; 37; 445-51.
15. Chuang WH, Lin SC, Chen SH, Wang CW, Tsai WC, Chen YJ, et al. Biomechanical effects of disc degeneration and hybrid fixation on the transition and adjacent lumbar segments: trade-off between

junctional problem, motion preservation, and load protection. Spine. 2012; 37: E1488-97.

16. Chung TT, Hueng DY, and Lin SC. Hybrid strategy of two-level cervical artificial disc and intervertebral cage. Medicine (Baltimore). 2015; 94: e2048.
17. Faizan A, Goel VK, Garfin SR, Bono CM, Serhan H, Bivani A, et al. Do design variations in the artificial disc influence cervical spine biomechanics? A finite element investigation, Eur Spine J. 2012; 21: S653-62.
18. Kallemeyn N, Gandhi A, Kode S, Shivanna K, Smucker J, Grosland N. Validation of a C2-C7 cervical spine finite element model using specimen-specific flexibility data. Med Eng Phys. 2010; 32: 482-9.
19. Jung TG, Woo SH, Park KM, Jang JW, Han DW, Lee SJ. Biomechanical behavior of two different cervical total disc replacement designs in relation of concavity of articular surfaces: ProDisc-C vs. Prestige-LP. Int. J. Precis. Eng. Manuf. 2013; 14: 819-24.
20. Ruberté LM, Natarajan RN, Andersson GB. Influence of single-level lumbar degenerative disc disease on the behavior of the adjacent segments—A finite element model study. J Biomech. 2009; 42: 341-8.
21. Kim K, Kim YH, Lee S. Investigation of optimal follower load path generated by trunk muscle coordination. J Biomech. 2011; 44: 1614-7.
22. Chuang WH, Kuo YJ, Lin SC, Wang CW, Chen SH, Chen YJ, et al. Comparison among load-, ROM-, and displacement-controlled methods used in the lumbo-sacral non-linear finite-element analysis. Spine. 2013; 38: E276-85.